



# Blinking adaptation for synchronizing a mobile agent network\*

Huan SHI<sup>†</sup>, Hua-ping DAI<sup>†‡</sup>, You-xian SUN

(State Key Laboratory of Industrial Control Technology, Zhejiang University, Hangzhou 310027, China)

<sup>†</sup>E-mail: {hshi, hpai}@iipc.zju.edu.cn

Received Sept. 27, 2010; Revision accepted Mar. 14, 2011; Crosschecked July 6, 2011

**Abstract:** We investigate the issue of synchronizing a blinking coupling mobile agent network through a blinking adaptation strategy, where each agent with blinking wave emission behavior not only adjusts its blinking period according to the local property of its neighbors, but also coordinates its blinking phase with those of neighboring agents. In leading the agents to blink orderly with a blinking period commensurate with the characteristic time of the dynamical oscillator, the presented blinking adaptation strategy works effectively in guaranteeing the synchronous motion of the considered network when the power density is large. In addition, the influence of the controlling parameter and moving velocity on network evolution is studied by assessing the convergence time.

**Key words:** Mobile agents, Blinking adaptation, Coupled-oscillator networks, Synchronization

**doi:**10.1631/jzus.C1000338

**Document code:** A

**CLC number:** TP13

## 1 Introduction

In the past decade, network-based approaches have attracted an increasing interest and have been proved to be prominent candidates to investigate the collective dynamics in many branches of science and engineering (Boccaletti *et al.*, 2002; 2006; Barabási, 2009). As a typical collective motion, synchronization in complex dynamical networks has been extensively studied. Many studies have pointed out that topological structure plays a significant role in the formation of network synchronization (Pecora and Carroll, 1998; Wen *et al.*, 2007; Arenas *et al.*, 2008). Thus far, synchronized behaviors have been studied mostly in the limit of static networks; i.e., the topological structures do not change as time evolves. Obviously, these static connection topologies do not

fit most realistic network systems; e.g., in biological networks, epidemiological networks, communication networks as well as social networks, the connection topology of the network generally changes in time. Therefore, researchers have recently devoted their efforts to time-varying complex networks (Belykh IV *et al.*, 2004; Belykh VN *et al.*, 2004; Skufca and Bollt, 2004; Lu and Chen, 2005; Frasca *et al.*, 2006; Chen, 2007; Wu, 2008; Qin *et al.*, 2009; Zhang *et al.*, 2010). Particularly, taking into account the co-evolution of dynamics states and network structures, many adaptive networks have been proposed and the corresponding synchronization issues have been intensively investigated (Zhou and Kurths, 2006; Wang and Sun, 2009; Zhu *et al.*, 2010).

In this paper, we focus our discussion on the synchronization issue in a power-driven mobile agent network (Shi *et al.*, 2010). Since this type of agent network has a remarkable feature of switching topology, it could be used as a good representation to explore many kinds of real-world problems, e.g., synchronous motion in clock of mobile robots (Buscarino

<sup>‡</sup> Corresponding author

\* Project supported by the National Natural Science Foundation of China (Nos. 60736021, 61004106, and U0735003) and the National High-Tech R & D Program (863) of China (No. 2009AA04Z154)

©Zhejiang University and Springer-Verlag Berlin Heidelberg 2011

et al., 2006), bulk oscillations of yeast cells (Dano et al., 1999), and collective reaction of a group of animals (Peng et al., 2009). Different from the existing agent network models (Frasca et al., 2008; Wang and Sun, 2009; Shi et al., 2010; Wang et al., 2010a; 2010b), we assign each agent a blinking emission power, so as to establish a blinking coupling mechanism, which can be used to characterize the intermittent influence capabilities of the mobile agents. It has been found that the intermittency feature of influence capabilities widely exists in individuals of real-world systems. For instance, in firefly flashing (Lewis and Cratsley, 2008), fireflies emit rays during one time interval and enter the non-luminous state in the following interval. In wireless sensor networks (Hart and Martinez, 2006), sensors are generally in the non-transmission state for energy efficiency, and switch to the transmission state only when needed.

Based on the moving agent network with blinking coupling structure, we propose a blinking adaptive rule to guarantee its synchronous behavior. The general idea behind the adaptation strategy covers two aspects: one is to regulate the blinking period of each agent to a proper common value according to the local synchronization property, and the other is to coordinate the blinking phase of each agent with those of its neighbors. In the following sections, we will show that when power density is large, synchronization of the considered network can be effectively guaranteed under the blinking adaptation strategy. In addition, by assessing the convergence time, we investigate the influence of the controlling parameter and moving velocity on network synchronization.

## 2 Blinking coupling mobile agent network

Consider a set of  $N$  moving agents, denoted by agent  $i$ ,  $i = 1, 2, \dots, N$ . Agent  $i$  is assigned to be equipped with a chaotic oscillator  $\mathbf{x}_i(t) \in \mathbb{R}^n$ , which is used to characterize the dynamical state agent  $i$ . Assume that all the agents move randomly in a two-dimensional plane. The plane satisfies periodic boundary conditions and is of linear size  $L$ . The positions and orientations of agents are evolving according to

$$\begin{cases} \mathbf{y}_i(t + \Delta t) = \mathbf{y}_i(t) + \mathbf{v}_i(t)\Delta t, \\ \theta_i(t + \Delta t) = \eta_i(t + \Delta t), \end{cases} \quad (1)$$

where  $\mathbf{y}_i(t)$  is the position of agent  $i$  in the plane at time  $t$ ,  $\mathbf{v}_i(t)$  with constant module (denoted by  $v$ ) and direction angle  $\theta_i(t)$  is the velocity of agent  $i$ ,  $\eta_i(t)$ ,  $i = 1, 2, \dots, N$  are  $N$  independent variables chosen randomly from the region  $[-\pi, \pi]$  according to uniform probability, and  $\Delta t$  is the time unit.

First of all, we recall the power-driven mechanism (Shi et al., 2010; Wang et al., 2010b) to establish directed connections among the mobile agents. Each agent is regarded to be a wave source with emission power  $P_e^i$ , which reads

$$P_e^i = 4\pi d^2 S^i(d), \quad S^i(d) \geq S_c, \quad (2)$$

where  $d$  indicates the distance from agent  $i$ ,  $S^i(d)$  as a function of  $d$  is the intensity of wave emitted by agent  $i$ , and  $S_c$  is a critical wave intensity. If the intensity of wave is beyond  $S_c$ , then agents can perceive it accurately. If agent  $i$  has emission power  $P_e^i$ , then there exists an influence radius, denoted by  $R_i = \sqrt{P_e^i/(4\pi S_c)}$ , within which  $S^i(d) \geq S_c$ . That is, directed couplings from agent  $i$  to its neighboring agents will be established immediately when the neighboring ones move into its influence range. Note that once the emission powers of agents are settled, couplings among agents are determined merely by their relative geographical locations in the plane.

However, not only the relative positions of the agents, but also their intermittent influence capabilities, can have an effect on the switching coupling structure among them. One can easily find many cases in nature as well as in man-made systems where the intermittency feature of influence capabilities has direct impact on couplings among individuals; e.g., in firefly flashing, no signal can be perceived by the neighboring fireflies if the firefly does not emit rays, even though the fireflies are in close proximity to each other (Lewis and Cratsley, 2008). As well as in wireless sensor networks, even if the sensors are within the service area of each other, they still cannot establish communications among them when in idle mode (Hart and Martinez, 2006). In this paper, we introduce a blinking coupling mechanism in order to have a better depiction of the widely existing intermittency feature in individuals' influence capability. Concretely, agent  $i$  takes a counter  $C_i(t)$  which counts repeatedly from zero to a value of  $C_u$  as follows:

$$C_i(t + \Delta t) = C_i(t) + K_i(t), \quad (3)$$

where  $C_u$  is a positive constant. Once the value of  $C_i(t)$  equals  $C_u$ ,  $C_i(t)$  restarts counting from zero, and  $K_i(t)$  controls the blinking period. Denoting the blinking period of agent  $i$  by  $T_b^i$ , we then derive that  $T_b^i = C_u/K_i(t) \cdot \Delta t$ . Moreover, we define a duty ratio  $\psi$ . Agent  $i$  remains in idle mode as  $C_i(t)$  is lower than  $\psi C_u$ , and agent  $i$  switches to emission mode when  $C_i(t)$  counts to larger than  $\psi C_u$ . During the period of idle mode, wave emission of agent  $i$  is turned off, and then, even if the other agents locate inside the influence range of agent  $i$ , they still cannot obtain information from agent  $i$ , which is very different from the case in Shi et al. (2010). As agent  $i$  switches from the idle mode to emission mode, wave emission is then turned on. Under such circumstances, coupling establishment among agents is the same as that in Shi et al. (2010). That is, when the relative distance between agent  $i$  and its surrounding agents is shorter than  $R$ , directed coupling will immediately be constructed from agent  $i$  to these agents. For simplicity, we consider that all the agents possess identical emission power, denoted by  $P$ ; i.e., each agent has the same influence radius  $R = \sqrt{P/(4\pi S_c)}$ . The following formula shows the blinking wave emission behavior of agent  $i$ :

$$P_e^i = \begin{cases} P, & nC_u \leq C_i(t) < \psi C_u + nC_u, \\ 0, & \text{otherwise,} \end{cases} \quad (4)$$

where  $n = 0, 1, \dots$  and  $i = 1, 2, \dots, N$ .

Under the blinking coupling rules, the mobile agents interact with each other and a dynamical network is thus constructed. Moreover, the mobile agent network can be formulated as follows:

$$\dot{\mathbf{x}}_i = \mathbf{f}(\mathbf{x}_i) - \sigma \sum_{j=1}^N g_{ij}(t) \mathbf{h}(\mathbf{x}_j), \quad (5)$$

where  $i = 1, 2, \dots, N$ ,  $\mathbf{f}(\cdot) : \mathbb{R}^n \rightarrow \mathbb{R}^n$  governs the local dynamics of the oscillator,  $\mathbf{h}(\cdot) : \mathbb{R}^n \rightarrow \mathbb{R}^n$  is a vectorial output function,  $\sigma > 0$  is the coupling strength, and time-varying Laplacian matrix  $\mathbf{G}(t) = (g_{ij}(t)) \in \mathbb{R}^{N \times N}$  describes the coupling relations among agents at time  $t$ . For the chaotic oscillator, without loss of generality, we consider the Rössler oscillator, whose state dynamics is described by:  $\dot{x}_{i1} = -(x_{i2} + x_{i3})$ ,  $\dot{x}_{i2} = x_{i1} + ax_{i2}$ ,  $\dot{x}_{i3} = b + x_{i3}(x_{i1} - c)$ , with  $\mathbf{x}_i = [x_{i1}, x_{i2}, x_{i3}]^T$  and  $a = 0.2, b = 0.2, c = 7.0$ , and we set  $\mathbf{h}(\mathbf{x}_i) = \mathbf{H}\mathbf{x}_i$ , where  $\mathbf{H} = \text{diag}\{1, 0, 0\}$ .

Note that time-varying Laplacian matrix  $\mathbf{G}(t)$  rests not only with the kinematics (mobility motion) of the agents, but also with the blinking wave emission behavior of each agent. Fig. 1 gives the coupling relation between two agents  $i$  and  $j$ . If the relative distance between  $i$  and  $j$  is larger than the influence radius  $R$ , then no matter  $i$  and  $j$  are in emission mode or not, no couplings can be established between them, i.e.,  $g_{ij}(t) = g_{ji}(t) = 0$ ; if agents  $i$  and  $j$  are in close proximity, within the influence radius of each other, then the blinking wave emission behavior governs the coupling structure. For specific details, if agent  $i$  is in emission mode and agent  $j$  in idle mode, then directed couplings can be established only from  $i$  to  $j$ , and no couplings exist from  $j$  to  $i$ , i.e.,  $g_{ij}(t) = 0, g_{ji}(t) = -1$ ; if agent  $j$  is in emission mode and agent  $i$  in idle mode, then directed couplings exist from  $j$  to  $i$ , and no couplings exist from  $i$  to  $j$ , i.e.,  $g_{ij}(t) = -1, g_{ji}(t) = 0$ ; if agents  $i$  and  $j$  are both in emission mode, then couplings from  $i$  to  $j$  and couplings from  $j$  to  $i$  exist simultaneously, i.e.,  $g_{ij}(t) = g_{ji}(t) = -1$ ; and if agents  $i$  and  $j$  are both in idle mode, then couplings from  $i$  to  $j$  and couplings from  $j$  to  $i$  disappear simultaneously, i.e.,  $g_{ij}(t) = g_{ji}(t) = 0$ .

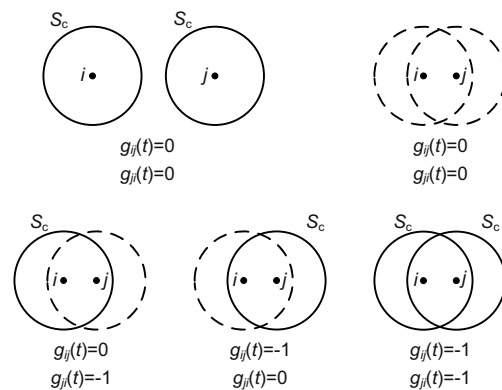


Fig. 1 Coupling relation between agents  $i$  and  $j$ , where the circle means the influence area, the dotted line implies the agent is in idle mode, while the solid line implies the agent is in emission mode

### 3 Synchronization analysis of the blinking coupling agent network

In the following, we will discuss the synchronous motion of network (5) under the blinking coupling mechanism. Since network (5) possesses random initial conditions and the mobility of the agents

also shows a random feature, we prefer to measure the synchronization process in a statistical way and further introduce two corresponding indexes: synchronization error  $\delta x(t)$  and synchronization index  $\langle \delta x \rangle$ . Synchronization error  $\delta x(t)$  is defined to be  $(\sum_{i=1}^N \|\mathbf{x}_i - \mathbf{x}_1\|)/N$  and synchronization index  $\langle \delta x \rangle$  is the average of  $\delta x(t)$  during the period  $[T, T + \Delta T]$ , where  $T$  is a sufficiently long evolving time. The parameters in simulations are set as:  $C_u = 2000$ ,  $\psi = 50\%$ ,  $T = 500$  s,  $\Delta T = 100$  s,  $\Delta t = 10^{-3}$  s,  $v = 1000$ , and each oscillator is assigned a random initial state which is around  $[1, 1, 1]^T$ .

For the case that the counters  $C_i(t)$  ( $i = 1, 2, \dots, N$ ) of agents are completely in a disordered state,  $K_i(t)$  are slightly different from each other and the values of  $C_i(t)$  are distributed in the region  $(0, C_u]$  according to uniform probability. In this case, network (5) switches among the possible topological configurations with high frequency as the agents move with sufficiently high velocity in the plane. And, at any moment, there are expected to be  $\psi N$  agents in emission mode. As a result, synchronous motion of network (5) is then guaranteed if the average network

$$\dot{\mathbf{x}}_i = \mathbf{f}(\mathbf{x}_i) - \sigma \sum_{j=1}^N \bar{g}_{ij} \mathbf{h}(\mathbf{x}_j) \quad (6)$$

can achieve synchronization (Stilwell *et al.*, 2006), where  $\bar{g}_{ij} = \frac{1}{T_w} \int_t^{t+T_w} g_{ij}(\tau) d\tau$ . According to the master stability function method (Pecora and Carroll, 1998) we learn that, when all the non-zero eigenvalues of the time-average Laplacian matrix  $\bar{\mathbf{G}} = (\bar{g}_{ij}) \in \mathbb{R}^{N \times N}$  locate in the region  $[\alpha_1/\sigma, \alpha_2/\sigma]$ , where  $\alpha_1$  and  $\alpha_2$  are positive constants, synchronous motion of network (6) can be guaranteed. Through matrix operation, we can obtain the eigenvalues of  $\bar{\mathbf{G}}$ , which reads:  $\lambda_1 = 0$ ,  $\lambda_2 = \dots = \lambda_N = NP\psi/(4S_c L^2)$ . Thus, under the case of disordered  $C_i(t)$ , network (5) is synchronizable if the power density of the agent network  $\rho_e = NP\psi/L^2$  locates in the bounded interval  $[\rho_{e1}, \rho_{e2}]$ , where  $\rho_{e1} = 4S_c \alpha_1/\sigma$ ,  $\rho_{e2} = 4S_c \alpha_2/\sigma$ . This result indicates that, under the case that the agents emit waves with disordered blinking behaviors, synchronization of the considered network cannot be achieved when the power density  $\rho_e$  is larger than the upper bound  $\rho_{e2}$ .

Next, we concentrate our attention on the case that all the counters perform orderly, i.e.,  $K_1(t) = \dots = K_N(t) = K$  ( $T_b^1 = \dots = T_b^N = T_b$ ) and

$C_i(t) = \dots = C_N(t)$ . Under this ordered case, the topology of the whole network possesses a fast-switching feature during the emission mode, and a totally disconnected graph can be used to describe it when idle mode dominates the network. The frequency by which network (5) switches between the two states depends on the value of  $K$ . If  $K$  is very large, then the fast-switching condition is satisfied. Thus, network (5) cannot achieve synchronization when the power density  $\rho_e$  is larger than  $\rho_{e2}$ . If  $K$  is very small, then both emission mode and idle mode will be sufficiently long. A power density beyond the upper bound  $\rho_{e2}$  will result in anarchy of network states during the long emission mode. In the following idle mode, network (5) still cannot achieve synchronization since all agents evolve without any interactions under the totally disconnected topology. Hence, for a power density larger than  $\rho_{e2}$ , network (5) cannot achieve synchronization either. The dividing value of a large  $K$  and a small  $K$  is closely related to the characteristic time of the dynamical unit, i.e., the Rössler oscillator. Fig. 2 gives the Fourier transformation of the Rössler oscillator. The Rössler oscillator possesses a dominant frequency  $f_c \approx 0.17$  Hz. That is to say, the order of magnitude of the characteristic time of the Rössler oscillator is 1 s. Fig. 3 shows the synchronization error  $\delta x(t)$  of network (5) evolving with time  $t$  under different values of  $K$ , where the other parameters are set as  $N = 100$ ,  $P = 3.14$ ,  $S_c = 1/4$ ,  $\rho_e = 1.5$ , and  $\sigma = 10$ . When  $K = 10$ , we obtain blinking period  $T_b = 0.2$  s, which is one order of magnitude smaller than the characteristic time of the Rössler oscillator, and when  $K = 0.1$ , we derive  $T_b = 20$  s, which is larger than the characteristic time of the Rössler oscillator by one order of magnitude. Since  $\rho_e = 1.5 > \rho_{e2}$ , we can find from Fig. 3 that, under the cases  $K = 0.1$  and  $K = 10$ , synchronization error  $\delta x(t)$  increases monotonically as time  $t$  evolves, indicating that synchronization cannot be achieved for network (5), which is consistent with the analytical results. When  $K = 1$ , i.e., the blinking period  $T_b = 2.0$  s, which has the same order of magnitude as the characteristic time of the Rössler oscillator, however, synchronous evolution is very different from that in the cases of  $K = 0.1$  and  $K = 10$ . From Fig. 3, synchronization error  $\delta x(t)$  decreases gradually as time  $t$  increases, implying the successful achievement of synchronization for network (5).

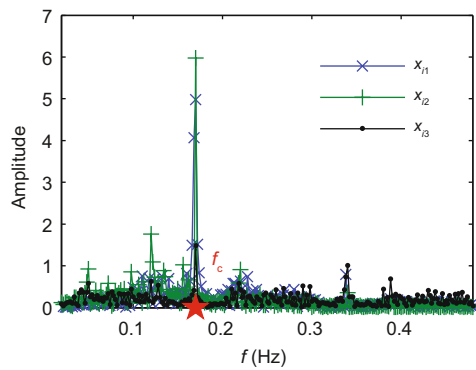


Fig. 2 Fourier transformation of the Rössler oscillator

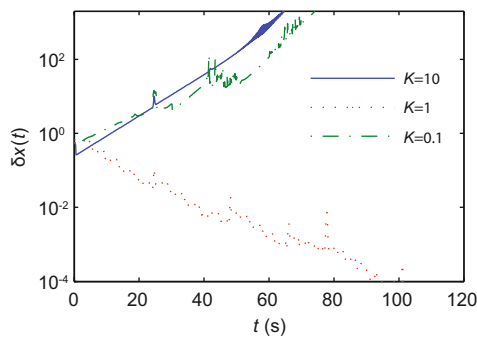


Fig. 3 Synchronization error  $\delta x(t)$  evolving with time  $t$  under ordered blinking behavior with a different blinking period  $T_b$ . The other parameters are set as  $N = 100$ ,  $P = 3.14$ ,  $S_c = 1/4$ ,  $\rho_e = 1.5$ , and  $\sigma = 10$

Moreover, for network (5) with blinking period  $T_b = 2.0$  s, which is commensurate with the characteristic time of the Rössler oscillator, we conduct a simulation to compare the synchronous motion of network (5) under both ordered and disordered blinking behaviors. Fig. 4 gives the results of synchronization error  $\delta x(t)$  evolving with time  $t$ , where the other simulation parameters are set the same as in Fig. 3. From the figure, we can see that, though the time scale of the blinking period has the same order of magnitude as that of the Rössler oscillator, network (5) achieves synchronization under the ordered blinking case, while anarchy prevails for network (5) under the disordered blinking case. Furthermore, the synchronization index  $\langle \delta x \rangle$  as a function of power density  $\rho_e$  under  $K = 1$  (i.e.,  $T_b = 2$  s) is reported in Fig. 5, where  $N = 100$ ,  $P = 3.14$ ,  $S_c = 1/4$ , and  $\sigma = 10$ . From Fig. 5, under the case of disordered blinking, anarchy prevails when  $\rho_e$  evolves out of the region  $[\rho_{e1}, \rho_{e2}]$ , which is consistent with the theoretical analysis. Under the case of ordered blinking, the synchronization index  $\langle \delta x \rangle$  remains at

zero when the power density  $\rho_e$  surpasses the upper bound  $\rho_{e2}$ ; i.e., the bounded synchronization region of power density reduces to an unbounded one.

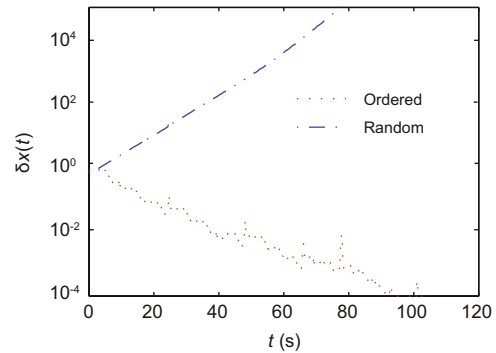


Fig. 4 Synchronization error  $\delta x(t)$  evolving with time  $t$  under disordered and ordered blinking behaviors, where blinking period  $T_b = 2.0$  s.  $N = 100$ ,  $P = 3.14$ ,  $S_c = 1/4$ ,  $\rho_e = 1.5$ , and  $\sigma = 10$

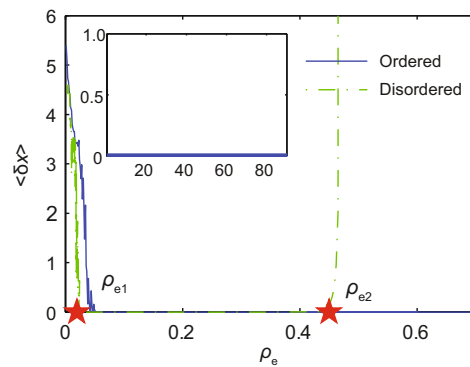


Fig. 5 Synchronization index  $\langle \delta x \rangle$  as a function of power density  $\rho_e$  under disordered and ordered blinking behaviors, respectively, with  $N = 100$ ,  $P = 3.14$ ,  $S_c = 1/4$ , and  $\sigma = 10$

From the analysis above, we can conclude that, when the power density  $\rho_e$  is larger than the upper bound  $\rho_{e2}$ , synchronization of network (5) can be achieved provided that the following two conditions are both satisfied: one is to make the agents blink orderly, and the other is to set the blinking period to be of the same order of magnitude as the characteristic time of the dynamical unit (Rössler oscillator). This result is quite different from the one derived in the blinking small-world network (Belykh IV *et al.*, 2004). The synchronization issue in the blinking small-world networks is very similar to that of the blinking coupling mobile agent network in the

disordered blinking case, while the slight difference between them is that, switching of topology in the blinking small-world network depends only on the blinking behavior, but switching of topology in the disordered blinking coupling mobile agent network depends not only on the blinking behavior of agents, but also on the mobility of agents. Therefore, the fast-switching condition is more easily satisfied in the disordered blinking coupling mobile agent network than in the blinking small-world network; i.e., even though the time scale of the blinking period increases to be of the same order of magnitude as that of the oscillator dynamics (Rössler oscillator), the fast-switching constraint can still be applied to investigate the corresponding synchronization issue of the disordered blinking coupling mobile agent network when agents move with high velocities. More importantly, in the blinking coupling mobile agent network, our novel finding is that, too short or too long a blinking period is not suitable in making the considered network achieve synchronization when the blinking behavior is in an ordered way, and the best choice is to set the blinking period to be in the same order of magnitude as the characteristic time of the dynamical unit. Compared with the case of fast-switching, synchronizability of the agent network is enhanced dramatically when the agents blink orderly with a blinking period commensurate with the characteristic time of the oscillator, and the bounded synchronization region of power density in the fast-switching case reduces to an unbounded one in the ordered blinking case with a proper blinking period. And, the result we obtain further provides a way to enhance the synchronizability of network (5) by leading the agents to blink in an orderly fashion with a proper frequency.

#### 4 Blinking adaptation strategy and discussions

Based on the analysis above, we here propose a simple scheme of blinking adaptation according to a local property to synchronize the considered network that possesses a power density  $\rho_e$  beyond  $\rho_{e2}$ . To make network (5) realize complete synchronization, we suppose that each agent adjusts its period and its counter value as the average period and the average counter value of its neighbors. Moreover, at every time step, each agent attempts to prolong its

blinking period if there exists a deviation between the state of itself and the mean state of its surrounding agents. Specifically, the counter  $C_i(t)$  of agent  $i$  evolves according to the following rule using all of the local information it can obtain:

$$\begin{cases} K_i(t + \Delta t) = \frac{1}{g_{ii}(t)} \sum_{j=1}^N g_{ij}(t) K_j(t) + \dot{K}_i(t) \Delta t, \\ C_i(t + \Delta t) = \frac{1}{g_{ii}(t)} \sum_{j=1}^N g_{ij}(t) C_j(t) + K_i(t), \end{cases} \quad (7)$$

where

$$\dot{K}_i(t) = \frac{-K_i(t)\gamma\Delta_i}{1 + \Delta_i}, \quad \Delta_i = \left\| \sum_{j=1}^N g_{ij}(t) \mathbf{h}(\mathbf{x}_j) \right\|^2, \quad (8)$$

the derivative of  $K_i(t)$  is used to restrain the difference  $\Delta_i$ , and controlling parameter  $\gamma > 0$  is used to regulate the speed of convergence.

As the blinking behavior of each agent evolves according to adaptive law (7)–(8), we consider the case of power density larger than  $\rho_{e2}$ , in which network (5) cannot achieve synchronization unless all the agents blink orderly with a common proper frequency. When each agent starts from a blinking behavior of high frequency and a random counter value, the fast-switching condition is satisfied for network (5). Therefore, anarchy will prevail in network (5) under  $\rho_e > \rho_{e2}$ . Then, according to adaptive law (7)–(8), the blinking period of each agent develops gradually; at the same time, all the agents tend to blink in an ordered way. After a short period, all the agents blink orderly with a proper frequency, which results in convergence of network (5). Note that, there needs to be a period of time for network (5) to achieve full synchronization. Thus, if the blinking period changes too rapidly to make the agents blink sufficiently slowly before network (5) achieves complete synchronization, divergence will reappear. Thus, we should manipulate the parameter  $\gamma$  to regulate the increment rate of the blinking period. A smaller  $\gamma$  implies slower increment of the blinking period; i.e., network (5) has a relatively long time to evolve from anarchy state to synchronous state. In the long term, all states of the network agents tend to converge to a synchronous orbit; i.e.,  $\Delta_i$  attenuates and the blinking period grows more and more slowly. When choosing a small value for  $\gamma$ , the blinking periods will finally converge to a common constant and

synchronous motion of network (5) is thus guaranteed. Fig. 6 reports synchronization error  $\delta x(t)$  vs. time  $t$  for different  $\gamma$ , where  $N = 100$ ,  $P = 3.14$ ,  $S_c = 1/4$ ,  $\rho_e = 1.5$ , and  $\sigma = 10$ . When  $\gamma$  possesses a small value ( $\gamma = 5$  and  $\gamma = 15$ ), synchronization of network (5) is achieved under the adaptation law (7)–(8), and anarchy prevails when  $\gamma$  is large ( $\gamma = 45$ ) (Fig. 6). The main trends of the curve  $\delta x(t)$  in the synchronization cases are almost the same: at the beginning,  $\delta x(t)$  grows as  $t$  evolves, since the fast-switching condition is satisfied, and thus the network has no synchronization trends; as time  $t$  goes further,  $\delta x(t)$  is prone to decrease since the proper blinking behavior is achieved by adaptive law (7)–(8). Finally synchronization error  $\delta x(t)$  vanishes, indicating that network (5) converges to a synchronous orbit. For the non-synchronization case,  $\delta x(t)$  shows a similar trend to that of the synchronization cases at the beginning phase, while in the convergence phase, the agents change the blink periods so rapidly that the blinking frequency becomes too low before complete synchronization is achieved, further resulting in anarchy of the network nodes' states once again.

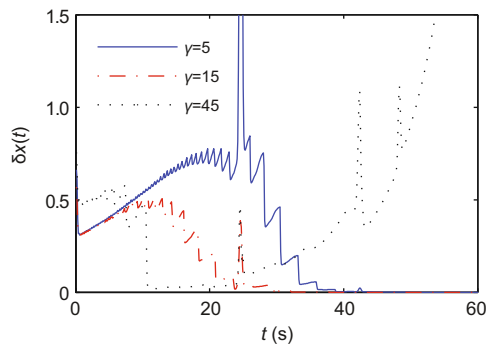


**Fig. 6** Synchronization error  $\delta x(t)$  vs. time  $t$  under different  $\gamma$  with  $N = 100$ ,  $P = 3.14$ ,  $S_c = 1/4$ ,  $\rho_e = 1.5$ , and  $\sigma = 10$

As a matter of fact,  $\gamma$  possesses a critical value  $\gamma_c$ , and we can guarantee the synchronous motion of network (5) under adaptive law (7)–(8) when  $\gamma < \gamma_c$ ; if  $\gamma > \gamma_c$ , divergence may occur as network (5) evolves according to law (7)–(8). We adopt a variable  $p_{\text{anarchy}}$  to describe the probability that anarchy prevails on network (5). Probability  $p_{\text{anarchy}}$  as a function of  $\gamma$  is reported in Fig. 7, where  $p_{\text{anarchy}}$  is numerically calculated through 100 conductions of simulation. From the figure, synchronization can be guaranteed for a small  $\gamma$ ; once  $\gamma$  surpasses the

threshold  $\gamma_c$ ,  $p_{\text{anarchy}}$  increases as  $\gamma$  evolves; when  $\gamma$  is sufficiently large, anarchy always prevails. The numerical analysis above guides us to choose a small value of  $\gamma$ , so that synchronous motion of network (5) can always be guaranteed.

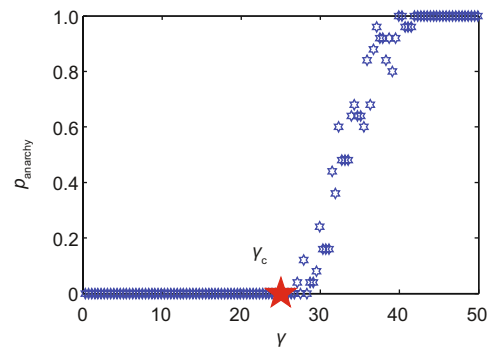


**Fig. 7** Probability  $p_{\text{anarchy}}$  vs. controlling parameter  $\gamma$  with  $N = 100$ ,  $P = 3.14$ ,  $S_c = 1/4$ ,  $\rho_e = 1.5$ , and  $\sigma = 10$

The discussions above show that controlling parameter  $\gamma$  plays a significant role in making network (5) realize synchronization. Here, we introduce convergence time  $T_c$  as a performance index to further evaluate the effect of  $\gamma$ . In detail,  $T_c$  is defined to be the total time from the beginning to the moment full synchronization of network (5) is achieved (in simulations, when  $\delta x(t) < 10^{-4}$ , network (5) is regarded to synchronize). Generally speaking, a shorter convergence time  $T_c$  is preferred for real-world systems (Sundaraman *et al.*, 2005). Fig. 8 gives the convergence time  $T_c$  vs. the parameter  $\gamma$ , where  $N = 100$ ,  $P = 3.14$ ,  $S_c = 1/4$ ,  $\rho_e = 1.5$ , and  $\sigma = 10$ .  $T_c$  shows as a concave function of  $\gamma$ . That is to say, an optimal value  $\gamma^o$  exists for network (5), and  $T_c$  achieves minimum under  $\gamma^o$ . Also, notice that a large  $\gamma$  will lead the network to a non-synchronization state— $T_c$  approaches infinity more and more quickly as  $\gamma$  increases. A small  $\gamma$  will result in a considerable convergence time though it can guarantee synchronous motion of the network. Therefore, we should choose a proper value of  $\gamma$  according to desirable performance, not too large or too small. In addition, we report the result of convergence time  $T_c$  evolving with the parameter  $\rho_e$  in Fig. 9, where  $N = 100$ ,  $P = 3.14$ ,  $S_c = 1/4$ ,  $\gamma = 5$ , and  $\sigma = 10$ .  $T_c$  is a finite constant for any particular  $\rho_e$ , indicating that complete synchronization of network (5) can be achieved by adaptation law (7)–(8) under any particular  $\rho_e$ .

$T_c$  increases with  $\rho_e$  at the beginning, and after  $\rho_e$  increases across about 2.5,  $T_c$  does not vary with  $\rho_e$  any more, nearly remaining constant.

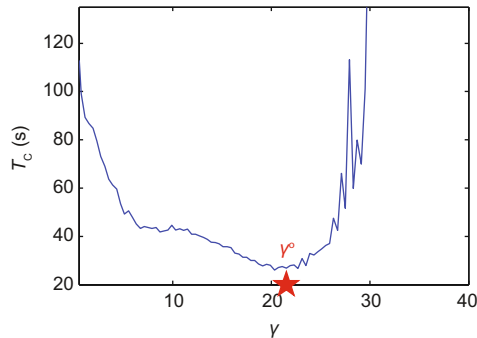


**Fig. 8** Convergence time  $T_c$  vs. controlling parameter  $\gamma$  with  $N = 100$ ,  $P = 3.14$ ,  $S_c = 1/4$ ,  $\rho_e = 1.5$ , and  $\sigma = 10$

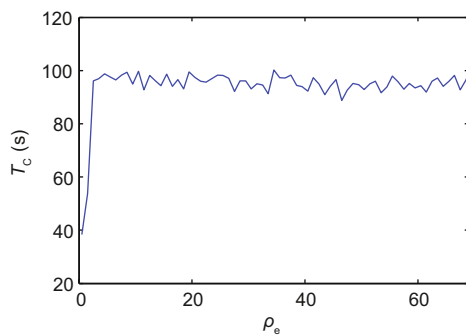


**Fig. 9** Convergence time  $T_c$  vs. power density  $\rho_e$  with  $N = 100$ ,  $P = 3.14$ ,  $S_c = 1/4$ ,  $\gamma = 5$ , and  $\sigma = 10$

In previous discussions, we assume that agents in network (5) move with a high velocity. We have carried out simulations to study the effect of the kinematics of agents on the synchronization performance of network (5). Fig. 10 reports the index  $T_c$  vs. moving velocity  $v$  under different  $\gamma$ , where  $N = 100$ ,  $P = 3.14$ ,  $S_c = 1/4$ ,  $\rho_e = 1.5$ , and  $\sigma = 10$ . For network (5) with  $\gamma = 5$ , there seems to be a threshold of  $v$ , denoted by  $v_c$ : if  $v > v_c$ , then  $T_c$  is almost a fixed constant; otherwise, the main trends of  $T_c$  is monotonically decreasing. This may be explained similarly by the reason provided by Skufca and Bolt (2004). As agents start from a low moving velocity, with the increase in  $v$ , interactions among agents become more and more frequent, further accelerating the convergence of the synchronization process. During this stage, system performance raises noticeably

as moving velocity increases. After the threshold value  $v_c$ , the fast-switching condition is satisfied and network (5) reduces to a fast-switching case. Moreover, lowering  $v$  can make network (5) with  $\gamma = 45$  synchronize again, as has been shown in Fig. 10 that  $T_c$  is a finite value for a small velocity, implying that synchronization of network (5) can be achieved; in the meantime, from Fig. 6, network (5) cannot achieve synchronization under  $\gamma = 45$  when velocity is high. For the case of  $\gamma = 45$ , it is also seen that network (5) possesses an optimal performance point in terms of  $T_c$ , and this optimal performance is realized provided that moving velocity  $v$  achieves an optimal value  $v^o$ . This phenomenon may also be explained through the speed of information exchange. Lowering  $v$  means slowing down the change rate of the blinking period, just like lowering the value of  $\gamma$ . Thus, synchronization can be achieved when choosing a small moving velocity.

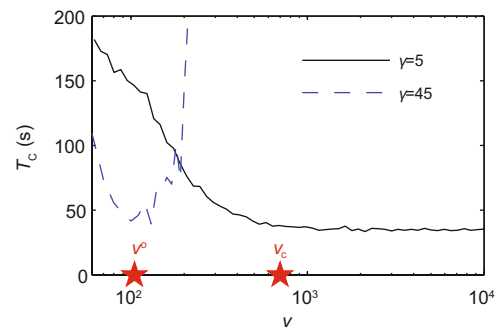


**Fig. 10** Convergence time  $T_c$  vs. velocity  $v$  with  $N = 100$ ,  $P = 3.14$ ,  $S_c = 1/4$ ,  $\rho_e = 1.5$ , and  $\sigma = 10$

## 5 Conclusions

A blinking coupling mechanism is introduced for the mobile agent network to characterize the intermittent influence capability of each agent; i.e., the agents are allotted blinking wave emission powers to build directed couplings among them. For this blinking coupling agent network, we suggest a blinking adaptive strategy to guarantee the corresponding synchronization motion. Theoretical analysis and numerical simulations have shown that the proposed blinking adaptive tactic is quite efficient in making the considered network achieve synchronization when the power density is large. We also discuss the impact of the controlling parameter and moving



velocity on network synchronization by assessing the convergence time. All these investigations may provide some insights for the future research work on synchronization enhancement in coupled oscillator networks and may also open up new possibility to design potential engineering applications, e.g., mobile sensor networks, moving robotics systems, as well as unmanned aerial vehicles.

## References

- Arenas, A., Diaz-Guilera, A., Kurths, J., Moreno, Y., Zhou, C.S., 2008. Synchronization in complex networks. *Phys. Rep.*, **469**(3):93-153. [doi:10.1016/j.physrep.2008.09.002]
- Barabási, A.L., 2009. Scale-free networks: a decade and beyond. *Science*, **325**(5939):412-413. [doi:10.1126/science.1173299]
- Belykh, I.V., Belykh, V.N., Hasler, M., 2004. Blinking model and synchronization in small-world networks with a time-varying coupling. *Phys. D*, **195**(1-2):188-206. [doi:10.1016/j.physd.2004.03.013]
- Belykh, V.N., Belykh, I.V., Hasler, M., 2004. Connection graph stability method for synchronized coupled chaotic systems. *Phys. D*, **195**(1-2):159-187. [doi:10.1016/j.physd.2004.03.012]
- Boccaletti, S., Kurths, J., Osipov, G., Valladares, D.L., Zhou, C.S., 2002. The synchronization of chaotic systems. *Phys. Rep.*, **366**(1-2):1-101. [doi:10.1016/S0370-1573(02)00137-0]
- Boccaletti, S., Latora, V., Moreno, Y., Chavez, M., Hwang, D.U., 2006. Complex networks: structure and dynamics. *Phys. Rep.*, **424**(4-5):175-308. [doi:10.1016/j.physrep.2005.10.009]
- Buscarino, A., Fortuna, L., Frasca, M., Rizzo, A., 2006. Dynamical network interactions in distributed control of robots. *Chaos*, **16**(1):015116. [doi:10.1063/1.2166492]
- Chen, M.Y., 2007. Synchronization in time-varying networks: a matrix measure approach. *Phys. Rev. E*, **76**(1):016104. [doi:10.1103/PhysRevE.76.016104]
- Dano, S., Sorensen, P.G., Hynne, F., 1999. Sustained oscillations in living cells. *Science*, **402**:320-322. [doi:10.1038/46329]
- Frasca, M., Buscarino, A., Rizzo, A., Fortuna, L., Boccaletti, S., 2006. Dynamical network model of infective mobile agents. *Phys. Rev. E*, **74**(3):036110. [doi:10.1103/PhysRevE.74.036110]
- Frasca, M., Buscarino, A., Rizzo, A., Fortuna, L., Boccaletti, S., 2008. Synchronization of moving chaotic agents. *Phys. Rev. Lett.*, **100**(4):044102. [doi:10.1103/PhysRevLett.100.044102]
- Hart, J.K., Martinez, K., 2006. Environmental sensor networks: a revolution in the earth system science? *Earth-Sci. Rev.*, **78**(3-4):177-191. [doi:10.1016/j.earscirev.2006.05.001]
- Lewis, S.M., Cratsley, C.K., 2008. Flash signal evolution, mate choice, and predation in fireflies. *Ann. Rev. Entomol.*, **53**:293-321. [doi:10.1146/annurev.ento.53.103106.093346]
- Lu, J.H., Chen, G.R., 2005. A time-varying complex dynamical network model and its controlled synchronization criteria. *IEEE Trans. Autom. Control*, **50**(6):841-846. [doi:10.1109/TAC.2005.849233]
- Pecora, L.M., Carroll, T.L., 1998. Master stability functions for synchronized coupled systems. *Phys. Rev. Lett.*, **80**(10):2109-2112. [doi:10.1103/PhysRevLett.80.2109]
- Peng, L.Q., Zhao, Y., Tian, B.M., Zhang, J., Wang, B.H., Zhang, H.T., Zhou, T., 2009. Consensus of self-driven agents with avoidance of collisions. *Phys. Rev. E*, **79**(2):026113. [doi:10.1103/PhysRevE.79.026113]
- Qin, S.M., Zhang, G.Y., Chen, Y., 2009. Coevolution of game and network structure with adjustable linking. *Phys. A*, **388**(23):4893-4900. [doi:10.1016/j.physa.2009.08.010]
- Shi, H., Wang, L., Dai, H.P., Sun, Y.X., 2010. Synchronization in a power-driven moving agent network. *Phys. A*, **389**(16):3094-3100. [doi:10.1016/j.physa.2010.03.042]
- Skufca, J.D., Boltt, E.M., 2004. Communication and synchronization in disconnected networks with dynamic topology: moving neighborhood networks. *Math. Biosci. Eng.*, **1**(2):347-359.
- Stilwell, D.J., Boltt, E.M., Roberson, D.G., 2006. Sufficient conditions for fast switching synchronization in time-varying network topologies. *SIAM J. Appl. Dyn. Syst.*, **5**(1):140-156. [doi:10.1137/050625229]
- Sundaraman, B., Buy, U., Kshemkalyani, A.D., 2005. Clock synchronization for wireless sensor networks: a survey. *Ad Hoc Networks*, **3**(3):281-323. [doi:10.1016/j.adhoc.2005.01.002]
- Wang, L., Sun, Y.X., 2009. Pinning synchronization of a mobile agent network. *J. Stat. Mech. Theory Exp.*, **2009**(11):P11005. [doi:10.1088/1742-5468/2009/11/P11005]
- Wang, L., Shi, H., Sun, Y.X., 2010a. Induced synchronization of a mobile agent network by phase locking. *Phys. Rev. E*, **82**(4):046222. [doi:10.1103/PhysRevE.82.046222]
- Wang, L., Shi, H., Sun, Y.X., 2010b. Power adaptation for a mobile agent network. *EuroPhys. Lett.*, **90**(1):10001. [doi:10.1209/0295-5075/90/10001]
- Wen, G., Wang, Q.G., Lin, C., Li, G.Y., Han, X., 2007. Chaos synchronization via multivariable PID control. *Int. J. Bifurc. Chaos*, **17**(5):1753-1758. [doi:10.1142/S0218127407018051]
- Wu, X.Q., 2008. Synchronization-based topology identification of weighted general complex dynamical networks with time-varying coupling delay. *Phys. A*, **387**(4):997-1008. [doi:10.1016/j.physa.2007.10.030]
- Zhang, X.S., Chen, T., Zheng, J., Li, H., 2010. Proactive worm propagation modeling and analysis in unstructured peer-to-peer networks. *J. Zhejiang Univ.-Sci. C (Comput. & Electron.)*, **11**(2):119-129. [doi:10.1631/jzus.C0910488]
- Zhou, C.S., Kurths, J., 2006. Dynamical weights and enhanced synchronizability in adaptive complex networks. *Phys. Rev. Lett.*, **96**(16):164102. [doi:10.1103/PhysRevLett.96.164102]
- Zhu, J.F., Zhao, M., Yu, W.W., Zhou, C.S., Wang, B.H., 2010. Better synchronizability in generalized adaptive networks. *Phys. Rev. E*, **81**(2):026201. [doi:10.1103/PhysRevE.81.026201]